The case of a crystal of finite thickness was dealt with by Litzman & Rózsa (1990). The dispersion equation (2.17) is the same but the formula for the intensity does not have the simple form (2.20).

In the case of a crystal with s atoms in the basis the dispersion equation has a more complicated form (Litzman, 1986):

$$\det \left\| I - C - \sum_{pq} (\{\exp[i(\theta^{-}_{pq} - \psi)] - 1\}^{-1} B_{pq} + \{\exp[-i(\theta^{+}_{pq} - \psi)] - 1\}^{-1} D_{pq}) \right\|, \qquad (4.1)$$

where I, C, B_{pq} and D_{pq} are matrices of order s. Neither the dispersion equation (4.1) nor the formulae for the intensities of the reflected and transmitted waves have been analyzed yet.

The dispersion equation for the diffraction of light on a periodic system of dipoles has a form similar to (4.1) (Litzman, 1978, 1980).

We think that a more profound study of the exact Ewald analytical formulae would be useful to test different approximations used in Bethe–Laue's conventional and extended dynamical theory, not only for neutrons but also for X-rays, as was shown for simple examples in Litzman & Dub (1990) and Litzman & Rózsa (1990).

References

AFANAS'EV, A. M. & MELKONYAN, M. K. (1983). *Acta Cryst.* A**39**, 207–210.

AVRON, J. E., GROSSMAN, A. & HØEGH-KROHN, R. (1983). *Phys. Lett. A*, **94**, 42–44.

BEDYŃSKA, T. (1974). *Phys. Status Solidi A*, **25**, 405–411.

BETHE, H. (1928). *Ann. Phys. (Leipzig)*, **87**, 55–129.

BRÜMMER, O., HÖCHE, H. R. & NIEBER, J. (1979). *Phys. Status Solidi A*, **53**, 565–570.

DEDERICHS, P. H. (1972). *Dynamical Diffraction Theory by Optical Potential Method Solid State Physics*, Vol. 27, edited by H. EHRENREICH, F. SEITZ & D. TURNBULL, pp. 135–236. New York: Academic Press.

EWALD, P. P. (1916). *Ann. Phys. (Leipzig)*, **49**, 1–38, 117–143.

EWALD, P. P. (1917). *Ann. Phys. (Leipzig)*, **54**, 519–597.

HÄRTWIG, J. (1977). *Phys. Status Solidi A*, **42**, 495–500.

JAMES, R. W. (1963). *The Dynamical Theory of X-ray Diffraction. Solid State Physics*, Vol. 15, edited by F. SEITZ & D. TURNBULL, p. 61. New York: Academic Press.

LAUE, M. (1948). *Materiewellen und ihre Interferenzen.* Leipzig: Akademische Verlagsgesellschaft.

LAX, M. (1951). *Rev. Mod. Phys.* **23**, 287–310.

LITZMAN, O. (1978). *Opt. Acta*, **25**, 509–526.

LITZMAN, O. (1980). *Opt. Acta*, **27**, 231–240.

LITZMAN, O. (1986). *Acta Cryst.* A**42**, 552–559.

LITZMAN, O. & DUB, P. (1990). *Acta Cryst.* A**46**, 247–254.

LITZMAN, O. & RÓZSA, P. (1990) *Acta Cryst.* A**46**, 897–900.

RAUCH, H. & PETRASCHECK, D. (1978). *Dynamical Neutron Diffraction and its Application. Topics in Current Physics*, Vol. 6, *Neutron Diffraction*, edited by H. DACHS, pp. 303–351. Berlin: Springer-Verlag.

SEARS, V. F. (1989). *Neutron Optics.* Oxford Univ. Press.

Acta Cryst. (1991). A**47**, 87–95

Perturbation Theory in High-Energy Transmission Electron Diffraction

BY J. M. ZUO

Department of Physics, Arizona State University, Tempe, AZ 85287, *USA*

(*Received* 3 *May* 1990; *accepted* 4 *September* 1990)

Abstract

A perturbation theory for many-beam high-energy transmission electron diffraction in noncentrosymmetric crystals is described for both the nondegenerate and degenerate cases. This perturbation theory differs from the conventional quantum-mechanical perturbation theory by perturbing the electron wavevectors instead of the total electron energy, which is constant for elastically scattered electrons. The relations between the perturbation theory and some other approximations commonly used in electron diffraction are discussed. It is shown that the few-beam approximation and the Kambe approximation are both applications of degenerate perturbation theory. Finally, as an example, this degenerate perturbation theory is applied to obtain an analytical solution to a four-beam case with two systematic (0 and g) and two nonsystematic (h and l) beams. This four-beam solution shows that the intensity of a four-beam interaction depends on all the four three-phase invariants involved, and also shows that the effects of the g beam on the three-beam interaction of 0, h and l are localized to the region near the Bragg condition of g. This may serve as a guide for future experiments using three-beam interactions for the measurement of structure-factor phases of an unknown structure.

1. Introduction

The formal theory of high-energy electron diffraction in a quantum-mechanical framework was established

0108-7673/91/020087-09$03.00

by Bethe in 1928. It was subsequently developed for transmission high-energy electron diffraction by several authors (for a review, see Humphreys, 1979). However, our understanding of dynamical diffraction effects, such as the intensity variation in a convergent-beam electron diffraction (CBED) disc, usually requires a large amount of numerical simulation by some algorithm based on the formal theory* (for example, see Zuo, Gjønnes & Spence, 1989), which does not give an intrinsic understanding which the explicit analytical solutions do. In past decades, various approximations have been developed and utilized to help us understand various effects of dynamical electron diffraction. These include the few-beam approximation, the Bethe second-order approximation, the Kambe approximation, the perturbation treatment of absorption and Buxton's perturbation treatment of high-order Laue-zone (HOLZ) effects. The few-beam approximation simplifies many-beam diffraction by only considering those beams which are strongly excited. The most commonly used few-beam approximation is the two-beam approximation, which can be solved analytically. For cases involving three or more beams, a transparent analytical solution is only possible when symmetries are contained in the diffraction configuration (Fukuhara, 1966). In this case valuable information can be obtained from analytical solutions (Gjønnes & Høier, 1971). The Bethe second-order approximation includes the effect of weak beams on the strong beams by introducing an effective potential. In the three-beam case it has been shown that the Bethe approximation is equivalent to the Kambe approximation (Kambe, 1957; Zuo, Høier & Spence, 1989). On the other hand, the Kambe strong coupling approximation is basically a degenerate perturbation treatment of three-beam electron diffraction as shown in this paper. The nondegenerate perturbation treatment of absorption by Hashimoto, Howie & Whelan (1962) and nondegenerate and degenerate perturbation treatment of HOLZ effects by Buxton (1976) follow the conventional quantum-mechanical approach in which a small potential perturbs the energy and wavefunction of the electron. This approach creates a conceptual difficulty since, in elastic diffraction, the electron has a constant total energy. It also leads to a specimen-thickness-dependent term due to the cross integration of two Bloch waves and the perturbation potential (this term cancels out in the two-beam case). A more suitable non-degenerate perturbation theory has been described by Wilkens, Katerbau & Ruhle (1973), Hussein & Wagenfeld (1978), Rez (1979) and Speer, Spence & Ihrig (1990). In these approaches, the *Anpassung* and eigenvectors are perturbed rather than the energy. In this paper, both nondegenerate and degenerate perturbation theory will be described for transmission electron diffraction. However, we will concentrate on the degenerate case, which has only been dealt with by Buxton (1976) in the conventional quantum-mechanical approach and is more useful in the many-beam diffraction cases. We will apply degenerate perturbation theory to a four-beam diffraction case to show the phase dependence of a four-beam interaction, and we will also use the four-beam results to study the validity of the three-beam approximation, which may be used in future experiments for the measurement of structure-factor phases of an unknown structure.

The practical importance of studying these approximations can be seen in their direct application to the study of crystal structure. Many approximations listed above have been used for the accurate measurement of structure-factor amplitudes and phases. For example, the critical voltage effect can be explained by the Bethe second approximation together with the two-beam approximation. The same combination can be used to explain systematic interactions (Gjønnes, Gjønnes, Zuo & Spence, 1988). Both the critical voltage effect and systematic interactions have been used to measure the structure factors of crystals accurately. [For examples of the application of the critical voltage effect, see Hewart & Humphreys (1974); for systematic interactions see Zuo, Spence & O'Keeffe (1988).] The same combination, when applied to noncentrosymmetric crystals, correctly explains the phase dependence of the three-beam interaction (Marthinsen, Matsuhata, Høier & Gjønnes, 1988) which, with the Kambe approximation, has been used to devise a method for accurate phase measurement using systematic and nonsystematic three-beam interactions in acentric crystals (Zuo, Spence & Høier, 1989; Zuo, Høier & Spence, 1989). Although these applications usually require a full many-beam dynamical simulation to obtain high accuracy, an approximation can greatly assist our basic understanding. Buxton's treatment of HOLZ effects provides the basic understanding of HOLZ patterns in the CBED pattern, which has been used to solve a crystal structure (Vincent, Bird & Steeds, 1984). These approximations may also play a more important role in solving the 'inversion problem' in the future. This 'inversion problem' refers to the problem of finding an unknown crystal structure from a set of electron diffraction patterns. The key to solving the 'inversion problem' is to find a set of simple parameters which can be directly related to structure factors and can be directly measured from a diffraction pattern (Gjønnes *et al.*, 1988). Numerical simulation cannot be applied in this case, because this requires prior knowledge of the structure. One possible inversion scheme occurs when the approximate crystal structure is known or the heavy-atom positions

* Except the symmetry of the CBED pattern, see Buxton, Eades, Steeds & Rackham (1976).

in the structure are known. In that case, strong dynamical interactions can be simulated, while the weak interactions (which are more sensitive to a small departure from the approximate structure or the light atoms) can be treated by perturbation theory, so an analytical formula for intensity can be obtained, which in turn can be inverted to find the structure factors. A practical case is the low-temperature monoclinic structure of magnetite (Fe_3O_4), which differs from the high-temperature cubic spinel structure by a very small atomic displacement and electron ordering on the octahedral site (Iizumi *et al.*, 1982 and references therein), which can be treated by perturbation (Zuo, Spence & Petuskey, 1990).

2. The Bloch wave theory of transmission high-energy electron diffraction (THEED)

The Bloch wave theory of dynamical electron diffraction was originally formulated by Bethe (1928). In this theory, the total wavefield inside a crystal is expanded in a basis of Bloch waves

$$\psi(\mathbf{r}) = \sum c_i \psi^i = \sum_i c_i \exp(2\pi i \mathbf{k}^i \cdot \mathbf{r}) \sum_g C_g^i \exp(2\pi i \mathbf{g} \cdot \mathbf{r}). \quad (1)$$

Expanding the potential of the crystal in the Fourier series, we have

$$U(\mathbf{r}) = \sum_g U_g \exp(2\pi i \mathbf{g} \cdot \mathbf{r}). \quad (2)$$

In this way, the Schrödinger equation becomes

$$[K^2 - (\mathbf{k}+\mathbf{g})^2] C_g + \sum_h U_{gh} C_h = 0. \quad (3)$$

Here K is the incident wavevector inside the crystal (k_0 outside the crystal), $K^2 = k_0^2 + U_0$, and k is the Bloch wavevector we are looking for. In principle, dynamical electron diffraction in a crystal can be solved by finding solutions of (3) and matching boundary conditions to find the excitation of each Bloch wave, the c_i. Diffraction by an arbitrary shape of crystal is too complicated to solve. The most common type of crystal shape we consider (as used in most experiments) is a parallel-sided thin slice. In this case, the tangential component of the incident wavevector is constant across the crystal surface. From the requirement of boundary condition, the tangential component of the wavevector is conserved inside and outside the crystal, so that

$$\mathbf{k}_t = \mathbf{K}_t = \mathbf{k}_{0t}. \quad (4)$$

With this condition, in general we can write

$$\mathbf{k} = \mathbf{K} + \gamma \mathbf{n}. \quad (5)$$

Equations (3) and (5) can be solved by diagonalizing a $2N \times 2N$ matrix to find the *Anpassung* γ and the eigenvectors $\{C_g\}$, which gives n forward-propagating Bloch waves and n backward Bloch waves (Collela, 1972). However, in the transmission case, the backscattering can be neglected so, in this case, $|\gamma| \ll K$. Thus we have

$$K^2 - (\mathbf{k}+\mathbf{g})^2 \simeq K^2 - (\mathbf{K}+\mathbf{g})^2 - 2(K_n + g_n)\gamma = 2KS_g - 2(K_n + g_n)\gamma. \quad (6)$$

Using the renormalization method (Lewis, Villagrana & Metherell, 1978), we define $B_g = (1 + g_n/K_n C_g)^{1/2}$, then (3) is simplified to

$$[2KS_g/(1+g_n/K_n)]B_g + \sum_h U_{gh}[(1+g_n/K_n)^{1/2}(1+n_n/K_n)^{1/2}]^{-1} B_h = 2K_n \gamma B_g. \quad (7)$$

Equation (7) can be solved by diagonalizing an $N \times N$ matrix. The only approximation made in deriving this equation is to neglect the backscattering, so it includes the HOLZ effects and specimen inclination effects and applies to noncentrosymmetric crystals. This equation has been used for calculations of CBED intensity in general situations (Zuo, Gjønnes & Spence, 1989). A similar formulation has also been used to study zone-axis HOLZ interactions (Jones, Rackham & Steeds, 1977). In the usual transmission case, the inclination of the crystal surfaces relative to the electron beam is small and we have $K_n \gg g_n$. So, to a good approximation, $g_n/K_n \simeq 0$, then

$$2KS_g C_g + \sum_h U_{gh} C_h = 2K_n \gamma C_g. \quad (8)$$

This equation gives n *Anpassung* γ^i and eigenvectors $\{C_g^i\}$ $(i = 1, \ldots, n)$. HOLZ effects are included approximately in (8). The crystal inclination effect is taken into account by $K_n = K \cos\theta$, where θ is the angle between the surface normal and the incident beam. The excitation coefficient c_i is found by matching the boundary conditions, which gives

$$\sum_i c_i C_0^i = 1.$$

For analytical simplicity, we will neglect absorption effects in this paper. In this case, we have

$$c_i = C_0^{i*}.$$

The intensity of beam g is given by

$$I_g = \left| \sum C_0^{i*} C_g^i \exp(2\pi i \gamma^i t) \right|^2. \quad (9)$$

Here t is the thickness of the crystal.

3. Perturbation theory in transmission high-energy electron diffraction

The idea of perturbation theory is to find the change in a known system, in this case a set of Bloch waves,

due to a small perturbation. The perturbation in electron diffraction could be a small change in the interaction parameter U_g or in the excitation error. In both cases, (8) is the most suitable starting point for our discussion. Equation (8) can be written in a matrix form

$$AC = \lambda C.$$

Here $A_{ii} = 2KS_g$ and $A_{ij} = U_{gh}$. Let $A = A_0 + A'$; A' is a small perturbation, resulting from a small change in U_g or in excitation error or both. Then,

$$A_0C + A'C = \lambda C.$$

The eigenvalues and eigenvectors of A_0 are τ_j and $\{\Gamma_i^j\}$, with $i, j = 1, \ldots, N$. (The symbols τ and Γ are used to avoid confusion with the λ and C of matrix A.) We write the eigenvector matrix of A as a combination of eigenvectors of A_0, $C = \Gamma\varepsilon$, where ε is the coefficient matrix and Γ is the eigenvector matrix of A_0 with $\Gamma_{ij} = \Gamma_i^j$. Then we have

$$\{\Gamma^{-1}A_0\Gamma + \Gamma^{-1}A'\Gamma\}\varepsilon = B\varepsilon = \lambda\varepsilon \qquad (10)$$

with

$$B_{ii} = \tau_i + b_{ii}$$

and

$$B_{ij} = b_{ij} = \sum_{km} \Gamma_{ik}^{-1}A'_{km}\Gamma_{mj} = \sum_{km} \Gamma_{ki}^{*}A'_{km}\Gamma_{mj}. \qquad (11)$$

3.1. *Nondegenerate perturbation*

The condition for no degeneracy is

$$|\tau_i - \tau_j| \gg |b_{\max}|. \qquad (12)$$

Here $|b_{\max}|$ is the largest element of b_{ij}, which can easily be shown to be of the same order as the largest element of the A' matrix. We are interested in effects of perturbation on the ith Bloch wave. We let

$$\lambda_i = \tau_i + \Delta,$$

where Δ is a small quantity of the same order as $|b_{\max}|$. With (12), we can neglect Δ and b_{ij} except for $j = i$. For the jth equation of (10), this leads to

$$(\tau_j - \tau_i)\varepsilon_{ji} + \sum_k b_{jk}\varepsilon_{ki} \simeq 0,$$

which gives

$$\varepsilon_{ji} \simeq b_{ji}/(\tau_i - \tau_j) \qquad (13)$$

with $\varepsilon_{ii} \simeq 1$, by normalization. Using this for the ith equation of (10), we find

$$\lambda_i = \tau_i + b_{ii} + \sum_j |b_{ij}|^2/(\tau_i - \tau_j). \qquad (14)$$

Equation (14) converges under condition (12). This shows the necessity for condition (12). Nondegenerate perturbation theory is useful in treating the absorption of crystals, in which case the small imaginary potential is treated as a perturbation. This approach was first used by Hashimoto, Howie & Whelan (1962) by perturbing the energy in the two-beam approximation. Strictly speaking, this is incorrect, since as stated in the *Introduction* the energy is constant for elastic electron scattering. However, in the two-beam case their results happen to agree with (14). In the general case with more than two beams, a perturbation of the energy leads to a thickness-dependent term which is not in (14) or (13) due to the integration of wavefunctions [see equation (9.17) in Hirsch, Howie, Nicholson, Pashley & Whelan, 1977). Furthermore, it is found that it is also necessary to include a correction to the eigenfunction of (13) in treating lattice defects (Wilkens, Katerbau & Ruhle, 1973; Rez, 1979) and absorption in acentric crystals (Spence & Zuo, 1990; Bird, 1990). The other application of nondegenerate perturbation is to include the weak-beam effects (Hussein & Wagenfeld, 1978; Eaglesham, 1989).

3.2. *Degenerate perturbation*

In most electron diffraction cases, many beams are excited. In these cases, we usually face a degenerate perturbation problem. In contrast to the nondegenerate case, we consider two Bloch waves to be degenerate when condition (12) is not satisfied. If the degeneracy is f fold, then the first-order wave function is to be found from

$$\begin{pmatrix} \tau_i - \lambda + b_{ii} & b_{ij} & \cdots & b_{ik} \\ b_{ji} & \tau_j - \lambda + b_{jj} & \cdots & b_{jk} \\ \vdots & \vdots & \cdots & \vdots \\ b_{ki} & b_{kj} & \cdots & \tau_k - \lambda + b_{kk} \end{pmatrix} \begin{pmatrix} \varepsilon_i \\ \varepsilon_j \\ \vdots \\ \varepsilon_k \end{pmatrix} = 0, \qquad (15)$$

where $\tau_i, \tau_j, \ldots, \tau_k$ are the *Anpassungs* of the f-degenerate Bloch waves. The general solution of (15) is impossible except when $f = 2$, that is only two Bloch waves are degenerate. In this case,

$$\begin{pmatrix} \tau_i - \lambda + b_{ii} & b_{ij} \\ b_{ji} & \tau_j - \lambda + b_{jj} \end{pmatrix} \begin{pmatrix} \varepsilon_i \\ \varepsilon_j \end{pmatrix} = 0. \qquad (16)$$

This gives

$$\lambda^{i,j} = \tfrac{1}{2}\{\tau_i + b_{ii} + \tau_j + b_{jj} \pm [(\tau_i + b_{ii} - \tau_j - b_{jj})^2 + 4|b_{ij}|^2]^{1/2}\} \qquad (17)$$

and

$$\varepsilon_{ii} = \cos(\beta/2)\exp(i\varphi), \quad \varepsilon_{ji} = \sin(\beta/2)$$
$$\varepsilon_{ij} = -\sin(\beta/2), \quad \varepsilon_{jj} = \cos(\beta/2)\exp(-i\varphi). \qquad (18)$$

Here φ is the phase of b_{ij} and β is defined by

$$\cot\beta = (\tau_i + b_{ii} - \tau_j - b_{jj})/2|b_{ij}|. \qquad (19)$$

In the following sections we will give some applications of degenerate perturbation theory in

transmission high-energy electron diffraction to show its importance.

4. Few-beam approximation and Kambe strong coupling approximation

The few-beam approximation has been widely used in electron diffraction for qualitative explanations, especially the two-beam approximation. However, the formal justification of this approximation is rarely seen in the literature. A justification of the few-beam approximation can be given on the basis of degenerate perturbation theory. We take A_0 to be a diagonal matrix with all the excitation errors on the diagonal and A' to be an off-diagonal matrix with interaction potential U_g,

$$A_0=\begin{pmatrix}0 & & & 0\\ & 2KS_g & & \\ & & 2KS_h & \\ 0 & & & \cdot\end{pmatrix},\qquad A'=\begin{pmatrix}0 & U_{-g} & U_{-h} & \cdot\\ U_g & 0 & U_{gh} & \cdot\\ U_h & U_{hg} & 0 & \cdot\\ \cdot & \cdot & \cdot & \cdot\end{pmatrix}. \tag{20}$$

In this case the zero-order solution is just plane waves with $\tau_i=2KS_g$ and $\Gamma_{ii}=1$, $\Gamma_{ji}=0$. A_0+A' is the ordinary scattering matrix. So from the results of the last section, those beams with excitation error $2KS_g$ of the order of U_g or smaller must be included, and those beams satisfying condition (12) can be neglected in the zero-order approximation.

The Kambe approximation refers to the approximation used by Kambe (1957) in studying structure-factor phase effects in nonsystematic three-beam (0, g and h) interactions as shown in Fig. 1. The condition for the Kambe approximation is that $|U_{gh}|\gg|U_g|$ or $|U_h|$. The Kambe approximation has been generalized to the many-beam case (Zuo, 1989). However, for simplicity we will look only at the three-beam case. In this case we take

$$A_0=\begin{pmatrix}0 & 0 & 0\\ 0 & 2KS_g & U_{gh}\\ 0 & U_{hg} & 2KS_h\end{pmatrix},\qquad A'=\begin{pmatrix}0 & U_{-g} & U_{-h}\\ U_g & 0 & 0\\ U_h & 0 & 0\end{pmatrix}. \tag{21}$$

The eigenvalues and eigenvectors of A_0 are

$$\tau_1=0,\qquad \tau_{2,3}=\tfrac{1}{2}\{S_g+S_h\pm[(S_g-S_h)^2+|U_{gh}/K|^2]^{1/2}\}, \tag{22}$$

$$\Gamma=\begin{pmatrix}1 & 0 & 0\\ 0 & \cos(\beta/2)\exp(i\varphi_{gh}) & -\sin(\beta/2)\\ 0 & \sin(\beta/2) & \cos(\beta/2)\exp(-i\varphi_{gh})\end{pmatrix}. \tag{23}$$

Using these results and (11), we obtain a simplified equation

$$\begin{pmatrix}\tau_1 & b_{12} & b_{13}\\ b_{21} & \tau_2 & 0\\ b_{31} & 0 & \tau_3\end{pmatrix}\begin{pmatrix}\varepsilon_1\\ \varepsilon_2\\ \varepsilon_3\end{pmatrix}=\lambda\begin{pmatrix}\varepsilon_1\\ \varepsilon_2\\ \varepsilon_3\end{pmatrix} \tag{24}$$

with

$$\begin{aligned}b_{12}&=U_{-g}\cos(\beta/2)\exp(i\varphi_{gh})\\ &\quad+U_{-h}\sin(\beta/2)\\ b_{12}&=-U_{-g}\sin(\beta/2)\\ &\quad+U_{-h}\cos(\beta/2)\exp(-i\varphi_{gh}).\end{aligned} \tag{25}$$

This is the same as the result obtained by Kambe (Kambe, 1957; Zuo, Høier & Spence, 1989). Equation (24) can be further simplified by considering the fact that, when $\tau_2\simeq 0$, $\tau_3\gg|b_{12}|$ or $|b_{13}|$ (or $\tau_3\simeq 0$, $\tau_2\gg|b_{12}|$ or $|b_{13}|$) due to the assumption $|U_{gh}|\gg|U_g|$ or $|U_h|$. The results of twofold-degenerate perturbation can then be applied. Detailed results have been given in the paper by Zuo, Høier & Spence (1989). These results are equivalent to the Bethe approximation where the Bethe approximation can be applied. This suggests the nature of perturbation in the Bethe approximation.

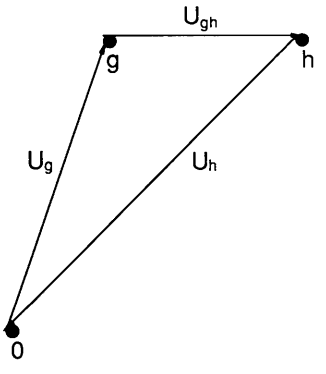

Fig. 1. A nonsystematic three-beam interaction with beams 0, g and h. This three-beam interaction can be treated by perturbation theory when $|U_{gh}|\gg|U_g|$ or $|U_h|$.

5. A four-beam solution without symmetry reduction

The degenerate perturbation theory described in § 3 can be readily applied to the four-beam case of Fig. 2. Such four-beam interactions usually exist in CBED patterns if nonsystematic three-beam interactions are established. (For example, see Fig. 2.) The exact solutions for the four-beam interactions have been obtained for a special case in centrosymmetric crystals when there is a mirror symmetry between the 0 and g and h and l reflections (Marthinsen *et al.*, 1988).

The results we present here are the approximate solutions for noncentrosymmetric crystals and for the general four-beam case. In studying four-beam interactions, we are mainly concerned about (i) the structure-factor phase dependence of four-beam interactions and (ii) the validity of the three-beam approximation. The second question has practical importance for attempts to solve unknown structures by directly measuring phases by electron diffraction. In that case, it is impossible to determine the phases by the three-beam refinement procedures used by Zuo, Høier & Spence (1989), since this method requires simulations of many-beam interactions, for which precise atomic coordinates are required. It is therefore preferable to use the three-beam or other analytical solutions which possess few parameters. By studying four-beam interactions, the validity of the three-beam approximation can also be studied quantitatively.

In the four-beam case of Fig. 2(a), we take

$$A_0=\begin{pmatrix}0 & U_{-g} & 0 & 0\\ U_g & 2KS_g & 0 & 0\\ 0 & 0 & 2KS_h & U_{hl}\\ 0 & 0 & U_{lh} & 2KS_l\end{pmatrix},$$
$$A'=\begin{pmatrix}0 & 0 & U_{-h} & U_{-l}\\ 0 & 0 & U_{gh} & U_{gl}\\ U_h & U_{hg} & 0 & 0\\ U_l & U_{lg} & 0 & 0\end{pmatrix}. \qquad (26)$$

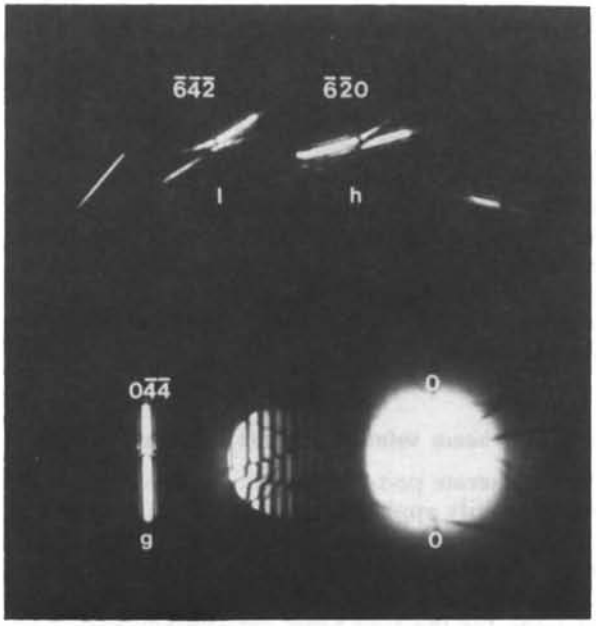

Fig. 2. An approximate experimental four-beam interaction with beams 0, g, h and l. This picture was taken at 100 kV from a crushed Si thin sample in a Philips 400T electron microscope.

In doing so, we assume

$$|U_g| \text{ or } |U_{hl}| \gg |U_h| \text{ or } |U_l| \text{ or } |U_{gh}| \text{ or } |U_{gl}|. \qquad (27)$$

This condition is a weak coupling condition. It divides the existing four reflections into two groups (0 and g) and (h and l) such that there is strong coupling within each group, but weak coupling between the two groups. The perturbation theory takes advantage of this weak coupling. This idea also works in the general many-beam case if the reflections can be divided into groups such that there is only weak coupling between reflections in different groups, but strong coupling between reflections in the same group. A practical example is provided by the nonsystematic case (Zuo, 1989) and HOLZ effects (Buxton, 1976).

The eigenvalues and eigenvectors of A_0 can be obtained easily. We find

$$\tau_{1,2}=\tfrac{1}{2}\{S_g \pm (S_g^2+|U_g/K_n|^2)^{1/2}\},$$
$$\tau_{3,4}=\tfrac{1}{2}\{S_h+S_l \pm [(S_h-S_l)^2+|U_g/K_n|^2]^{1/2}\} \qquad (28)$$
$$\Gamma=\begin{pmatrix}\cos\frac{1}{2}\beta\exp(-i\varphi_g) & -\sin\frac{1}{2}\beta & 0 & 0\\ \sin\frac{1}{2}\beta & \cos\frac{1}{2}\beta\exp(i\varphi_g) & 0 & 0\\ 0 & 0 & \cos\frac{1}{2}\alpha\exp(i\varphi_{hl}) & -\sin\frac{1}{2}\alpha\\ 0 & 0 & \sin\frac{1}{2}\alpha & \cos\frac{1}{2}\alpha\exp(i\varphi_{lh})\end{pmatrix}.$$

Here β and α are defined by $\cot\beta=-KS_g/|U_g|$ and $\cot\alpha=K(S_h-S_l)/|U_g|$. Using the above results and (11), we obtain the following equation:

$$\begin{pmatrix}\tau_1 & 0 & b_{13} & b_{14}\\ 0 & \tau_2 & b_{23} & b_{24}\\ b_{31} & b_{32} & \tau_3 & 0\\ b_{41} & b_{42} & 0 & \tau_4\end{pmatrix}\begin{pmatrix}\varepsilon_1\\ \varepsilon_2\\ \varepsilon_3\\ \varepsilon_4\end{pmatrix}=\lambda\begin{pmatrix}\varepsilon_1\\ \varepsilon_2\\ \varepsilon_3\\ \varepsilon_4\end{pmatrix}. \qquad (29)$$

Equation (29) is still too complicated to provide a general solution. It must be further simplified. To do that, let us look at the dispersion surface we expect from (29). The $\tau_{1,2}$ and $\tau_{3,4}$ give two sets of two-beam dispersion surfaces, which intersect with each other and give four intersection lines as shown in Fig. 3. This set of dispersion surfaces is called the asymptotic dispersion surface. Near each intersection, two Bloch waves are degenerate or almost degenerate. The introduction of the nonzero weak couplings [the b parameters in (29)] destroys the degeneracy and causes a hybridization of the dispersion surfaces, as predicted by (17). Fig. 4 shows a section of the four-beam dispersion surface taken on the plane Σ in Fig. 3, without coupling and with coupling. The conditions of (27) are used to guarantee that the gaps (such as

d in the figure) of the hybridization of the dispersion surfaces due to the weak coupling are small compared to the existing gaps (such as D in the figure) in other dispersion surfaces, as shown schematically in Fig. 4. In this case, away from the intersection, the dispersion surfaces rapidly approach the asymptotic dispersion surfaces. This is the basic assumption we have made in order to utilize perturbation theory in this case. In Fig. 5, the four intersection lines of the asymptotic surface in Fig. 3 are projected onto the CBED disc, together with the intersection lines of the zero plane with the g, h and l planes [the lines $K_g(S_g=0)$, $K_h(S_h=0)$ and $K_l(S_l=0)$] and the intersection lines of the g plane with the h and l planes (lines gh and gl). The four intersection lines in the CBED disc approach the lines K_h, K_l, gh and gl as shown in Fig. 5. Generally, with a relatively thick crystal we expect that along each intersection line there is a localized intensity maximum in the CBED disc (Zuo, 1989). In the following, we specifically look into parts 3 and 4 in the CBED disc of reflection 1 (see Fig. 5). Others can be similarly studied.

Part 4 is governed by intersection of τ_1 and τ_4. By neglecting the other two non-degenerate zero-order Bloch waves, we obtain

$$\begin{pmatrix} \tau_1-\lambda+b_{11} & b_{14} \\ b_{41} & \tau_4-\lambda+b_{44} \end{pmatrix}\begin{pmatrix} \varepsilon_1 \\ \varepsilon_4 \end{pmatrix}=0. \qquad (30)$$

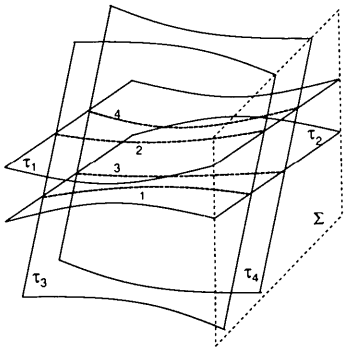

Fig. 3. An illustration of asymptotic four-beam dispersion surfaces given by two two-beam dispersion surfaces intersecting each other.

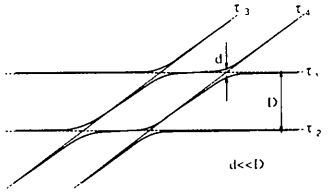

Fig. 4. A section of four-beam dispersion surfaces taken from plane Σ in Fig. 3. The dashed lines are the asymptotic dispersion. The full lines are the dispersion with the perturbation potential. The condition $d \ll D$ ensures that perturbation applies.

The solution of this type of equation is given by (17) and (18). With these solutions and (9), (11), (30) and $C=\Gamma\varepsilon$ we obtain an expression for the intensity in CBED due to τ_1 and τ_4 interaction as follows:

$$\begin{aligned} I_4 &= \cos^2(\beta/2)\cos^2(\alpha/2)\{|b_{14}|^2/[|b_{14}|^2+(KS_4)^2]\} \\ &\quad\times\sin^2(\pi t/K_n)[|b_{14}|^2+(KS_4)^2]^{1/2} \\ S_4 &= S_g+(S_g^2+|U_g/K|^2)^{1/2}-S_h-S_l \\ &\quad+[(S_h-S_l)^2+|U_{hl}/K|^2]^{1/2}+b_{11}-b_{44} \qquad (31) \\ |b_{14}|^2 &= |U_l|^2\cos^2(\alpha/2)\cos^2(\beta/2) \\ &\quad\times|\{1-(|U_h/U_l|)\tan(\alpha/2) \\ &\quad\times\exp[i(\varphi_{hl}+\varphi_l-\varphi_h)]\} \\ &\quad-(|U_{gh}/U_l|)\tan(\beta/2)\tan(\alpha/2) \\ &\quad\times\exp[i(\varphi_{gh}-\varphi_g+\varphi_{hl}+\varphi_l)] \\ &\quad+(|U_{gl}/U_l|)\tan(\beta/2) \\ &\quad\times\exp[i(\varphi_{gl}-\varphi_g+\varphi_l)]|^2 \\ b_{11} &= b_{44}=0. \end{aligned}$$

Similarly, for part 3 (Fig. 5)

$$\begin{aligned} I_3 &= \sin^2(\beta/2)\cos^2(\alpha/2)\{|b_{24}|^2/[|b_{24}|^2+(KS_3)^2]\} \\ &\quad\times\sin^2(\pi t/K_n)[|b_{24}|^2+(KS_3)^2]^{1/2} \\ S_3 &= S_g-(S_g^2+|U_g/K|^2)^{1/2}-S_h-S_l \\ &\quad+[(S_h-S_l)^2+|U_{hl}/K|^2]^{1/2} \qquad (32) \\ |b_{24}|^2 &= |U_l|^2\cos^2(\alpha/2)\sin^2(\beta/2)|\{1-|U_h/U_l| \\ &\quad\times\tan(\alpha/2)\exp[i(\varphi_{hl}+\varphi_l-\varphi_h)]\} \\ &\quad-|U_{gh}/U_l|\cot(\beta/2)\tan(\alpha/2) \\ &\quad\times\exp[i(\varphi_{gh}-\varphi_g+\varphi_{hl}+\varphi_l)] \\ &\quad-|U_{gl}|/|U_l|\cot(\beta/2) \\ &\quad\times\exp[i(\varphi_{gl}-\varphi_g+\varphi_l)]|^2. \end{aligned}$$

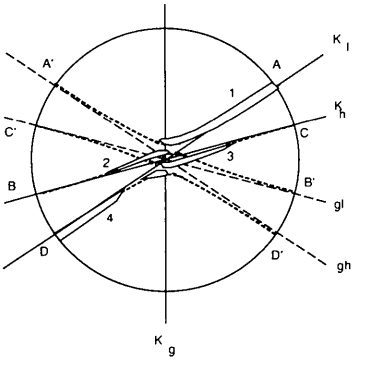

Fig. 5. The four intersection lines of asymptotic dispersion surfaces projected onto a CBED disc (see Fig. 3). Superimposed are the general intensity features that we expect from a four-beam interaction. The lines K_g, K_h and K_l are the Kikuchi lines of reflections g, h and l. For details, see text.

Of the quantities involved in both intensity expressions (31) and (32), only the effective potentials $|b_{14}|^2$ and $|b_{24}|^2$ depend on the phases. The four-phase invariant in (31) can be broken into two three-phase invariants,

$$\varphi_{gh} - \varphi_g + \varphi_{hl} + \varphi_l = (\varphi_{gh} - \varphi_g + \varphi_h) + (\varphi_{hl} + \varphi_l - \varphi_h).$$

So we conclude that the intensity in four-beam interactions depends on all four possible three-phase invariants. This is in contradiction with the conclusion of the second Bethe approximation, which gives a phase dependence

$$|U_l^{\text{eff}}|^2/|U_l|^2 = |1 - (|U_h||U_{hl}|/2K_nS_h|U_l|) \times \exp[i(\varphi_h - \varphi_l + \varphi_{hl})] - [|U_g||U_{gl}|/2K_nS_g|U_l|] \times \exp[i(\varphi_g - \varphi_l + \varphi_{gl})]|^2.$$

This only depends on the two three-phase invariants involving φ_1. The second Bethe approximation assumes that only two beams, 0 and l, are strongly excited and that both g and h are weak. In our approximation, all four beams can be strongly excited. It therefore describes the four-beam interaction more accurately than the Bethe approximation.

In the effective potential of $|b_{14}|^2$ and $|b_{24}|^2$ of (31) and (32), the terms within { } result from the three-beam (0, h and l) interactions (Zuo, Høier & Spence, 1989). The other terms within | | are due to the inclusion of a fourth beam g. The effects of the fourth beam are weighted by the factor $\tan(\beta/2)$ and $\cot(\beta/2)$ in $|b_{14}|^2$ and $|b_{24}|^2$, respectively. From the definition of $\cot\beta = -KS_g/|U_g| = -\omega$, we have

$$\tan(\beta/2) = 1/\cot(\beta/2) = (1+\omega^2)^{1/2} + \omega. \quad (33)$$

The functions $\tan(\beta/2)$ and $\cot(\beta/2)$ are plotted in Fig. 6. $\tan(\beta/2)$ decreases to zero when S_g becomes more negative and $\cot(\beta/2)$ decreases to zero when S_g becomes more positive. From line K_g to D' in Fig. 5, S_g is increasingly negative, and $\tan(\beta/2)$ in $|b_{14}|^2$ decreases to zero quickly and so does the effect of the fourth beam g. From line K_g to C', S_g is positive and increases, $\cot(\beta/2)$ in $|b_{24}|^2$ decreases to zero. So we may conclude that the disturbance due to the fourth beam g on the three-beam interaction 0, h and l is very localized to the region very close to the Bragg condition for g, the line K_g in Fig. 5. Away from that region, the intensity can be well described by the three-beam approximation. The size of the localized region depends on the sizes of g and U_g. The rule of thumb is that this region is about the same size as the bright area in the g disc.

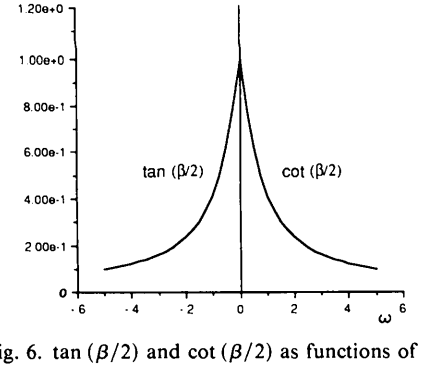

Fig. 6. $\tan(\beta/2)$ and $\cot(\beta/2)$ as functions of ω.

This work was supported by NSF grant no. DMR88-13879 and the NSF-Arizona State University National Center for High Resolution Electron Microscopy. The author acknowledges useful discussions with Professors J. C. H. Spence and R. Høier.

References

BETHE, H. A. (1928). *Ann. Phys. (Leipzig)*, **87**, 55-129.

BIRD, D. M. (1990). *Acta Cryst.* A**46**, 208-214.

BUXTON, B. F. (1976). *Proc. R. Soc. London Ser. A*, **350**, 335-361.

BUXTON, B. F., EADES, J. A., STEEDS, J. W. & RACKHAM, G. M. (1976). *Philos. Trans. R. Soc. London*, **281**, 171-193.

COLLELA, R. (1972). *Acta Cryst.* A**28**, 11-15.

EAGLESHAM, D. J. (1989). *Proc. 47th Annual Meeting of EMSA*, edited by G. W. BAILEY, pp. 482-483. San Francisco: San Francisco Press.

FUKUHARA, A. (1966). *J. Phys. Soc. Jpn*, **21**, 2645-2661.

GJØNNES, J. & HØIER, R. (1971). *Acta Cryst.* A**27**, 313-316.

GJØNNES, K., GJØNNES, J., ZUO, J. M. & SPENCE, J. C. H. (1988). *Acta Cryst.* A**44**, 810-820.

HASHIMOTO, H., HOWIE, A. & WHELAN, M. J. (1962). *Proc. R. Soc. London Ser. A*, **269**, 80-103.

HEWAT, E. A. & HUMPHREYS, C. J. (1974). In *High Voltage Electron Microscopy*, edited by P. R. SWANN *et al.*, p. 52. New York: Academic Press.

HIRSCH, P. S., HOWIE, A., NICHOLSON, R. B., PASHLEY, D. W. & WHELAN, M. J. (1977). *Electron Microscopy of Thin Crystals*. Florida: Robert E. Krieger.

HUMPHREYS, C. J. (1979). *Rep. Prog. Phys.* **42**, 1825-1887.

HUSSEIN, A. & WAGENFELD, H. (1978). *Electron Diffraction*: 1927-1977, edited by P. J. DOBSON *et al.*, p. 47-49. *Inst. Phys. Conf. Ser.* No. 41.

IIZUMI, M., KOETZLE, T. F., SHIRANE, G., CHIKAZUMI, S., MATSUI, M. & TODO, S. (1982). *Acta Cryst.* B**38**, 2121-2133.

JONES, P. M., RACKHAM, G. M. & STEEDS, J. W. (1977). *Proc. R. Soc. London Ser. A*, **354**, 197-222.

KAMBE, K. (1957). *J. Phys. Soc. Jpn*, **12**, 13-25.

LEWIS, A. L., VILLAGRANA, R. E. & METHERELL, A. J. F. (1978). *Acta Cryst.* A**34**, 138-139.

MARTHINSEN, K., MATSUHATA, H., HØIER, R. & GJØNNES, J. (1988). *Austr. J. Phys.* **41**, 449-459

REZ, P. (1979). *Phys. Status Solidi A*, **55**, K79-K82.

SPEER, S., SPENCE, J. C. H. & IHRIG, E. (1990). *Acta Cryst.* A**46**, 763-772.

SPENCE, J. C. H. & ZUO, J. M. (1990). Proc. XII Int. Congress for Electron Microscopy. Submitted.

VINCENT, R., BIRD, D. M. & STEEDS, J. W. (1984). *Philos. Mag.* **50**, 765-786.

WILKENS, W., KATERBAU, K. H. & RUHLE, M. (1973). *Z. Naturforsch. Teil A*, **28**, 681-690.

ZUO, J. M. (1989). *Proc. 47th Annual Meeting of EMSA*, edited by G. W. BAILEY, pp. 522-523. San Francisco: San Francisco Press.
ZUO, J. M., GJØNNES, K. & SPENCE, J. C. H. (1989). *J. Electron Microsc. Tech.* **12**, 29-55.
ZUO, J. M., HØIER, R. & SPENCE, J. C. H. (1989). *Acta Cryst.* A**45**, 839-851.
ZUO, J. M., SPENCE, J. C. H. & HØIER, R. (1989). *Phys. Rev. Lett.* **62**, 547-550.
ZUO, J. M., SPENCE, J. C. H. & O'KEEFFE, M. (1988). *Phys. Rev. Lett.* **61**, 353-356.
ZUO, J. M., SPENCE, J. C. H. & PETUSKEY, W. (1990). Proc. XII Int. Congress for Electron Microscopy, pp. 508-509.

Acta Cryst. (1991). A**47**, 95-101

Surface Superlattice Reflections and Kinematical Approximation in RHEED

BY L.-M. PENG AND M. J. WHELAN

Department of Materials, University of Oxford, Parks Road, Oxford OX1 3PH, England

(*Received* 17 *May* 1990; *accepted* 4 *September* 1990)

Abstract

The physical nature of the sharpness and weakness of surface superlattice spots in reflection high-energy electron diffraction (RHEED) and the validity of the kinematical approximation for analyzing the intensities of the superlattice spots are examined, using a Bloch-wave formulation of the dynamical theory of RHEED. It is found that although it is adequate to treat surface superlattice diffraction kinematically within the selvedge, a kinematical analysis of RHEED intensities of superlattice spots is not in general valid, unless some criteria are satisfied. These include a projection approximation for the superlattice in the selvedge, a glancing incidence such that no diffracted beams other than the incident and specularly reflected beams are excited in both the selvedge and the underlying bulk crystal.

1. Introduction

In recent years there has been a trend in the structure determination of reconstructed surfaces to use high-energy electron diffraction techniques, and to employ a kinematical approximation in analyzing the intensities of surface superlattice reflections (Takayanagi, Tanishiro, Takahashi & Takahashi, 1985*a*, *b*; Ino, 1977; Wu & Schowalter, 1988; Horio & Ichimiya, 1989). Theoretically this trend results from the intractability of carrying out dynamical calculations for large numbers of possible surface models and experimentally it is motivated by the great success of the determination of the dimer adatom stacking-fault (DAS) structure of the Si(111) 7×7 reconstructed surface using a simple kinematical analysis (Takayanagi *et al.*, 1985*a*, *b*).

While in the case of transmission electron diffraction (TED) the validity of the kinematical approximation has been examined using multislice calculations (Spence, 1983; Tanishiro & Takayanagi, 1989) for Si and certain incident-beam directions and analyzed using Bloch-wave theory (Peng & Whelan, 1991), far less has been done in the reflection high-energy electron diffraction (RHEED) case. Although it has long been realized that in RHEED electrons interact strongly with the atoms and dynamical calculations are needed, the extreme sharpness and weakness of the surface superlattice spots in RHEED patterns have been taken to suggest the validity of a kinematical description, *i.e.* the diffraction processes undergone by electrons associated with superlattice reflections are dominated by single-scattering processes. The intensities of superlattice spots in RHEED have therefore been analyzed kinematically (Ino, 1977; Wu & Schowalter, 1988; Horio & Ichimiya, 1989). It is the purpose of this paper to examine the various diffraction processes involved in both the selvedge and the underlying bulk crystal, within the framework of Bloch-wave dynamical theory, and to set criteria for the validity for the kinematical approximation in analyzing RHEED intensities of superlattice reflections.

2. General description

We shall consider a beam of high-energy electrons (10 keV or more, say) which is incident upon a flat surface at grazing incidence. Here the surface is thought of as consisting of a selvedge, over which there is a reconstruction, and the underlying bulk crystal. There are three distinct regions which need to be treated separately. For the vacuum region above the surface, there exist the incident electron beam and several reflected beams, and the total wavefunction may be written as

$$\psi_v(\mathbf{r}) = \exp(i\boldsymbol{\chi}.\mathbf{r}) + \sum_m R_m \exp(i\mathbf{K}_m.\mathbf{r}), \qquad (1)$$

0108-7673/91/020095-07$03.00